This is to certify that the

thesis entitled

THREE DIMENSIONAL VISUALIZATION OF
ELECTROMAGNETIC FIELDS AT RESONANCE
IN AN IDEAL UNLOADED CYLINDRICAL CAVITY

presented by

JOSHUA NATARAJAN

has been accepted towards fulfillment
of the requirements for

Master's degree in Electrical Eng

Marvin Siegel
Major professor

Date NOV 16, 1995

DATE DUE	DATE DUE	DATE DUE
JUN 1 1 [illegible] [illegible]		

THREE DIMENSIONAL VISUALIZATION OF ELECTROMAGNETIC FIELDS AT RESONANCE IN AN IDEAL UNLOADED CYLINDRICAL CAVITY

By

Joshua Natarajan

A THESIS

Submitted to
Michigan State University
in partial fulfillment of the requirements
for the degree of

MASTER OF SCIENCE

Department of Electrical Engineering

1995

ABSTRACT

THREE DIMENSIONAL VISUALIZATION OF ELECTROMAGNETIC FIELDS AT RESONANCE IN AN IDEAL UNLOADED CYLINDRICAL CAVITY

By

Joshua Natarajan

The resonant electric and magnetic fields in a cylindrical cavity have complex three dimensional trajectories that are not always easy to discern from two dimensional field plots. This thesis attempts to realize a user friendly environment to visualize these complex fields and their intensities in a three dimensional environment written in Microsoft Visual C++™ for the Microsoft Windows™ operating system.

ACKNOWLEDGMENTS

I would like to thank my advisor, Dr. Siegel for his generous support in helping me realize this idea. I would also like to thank Dr. Rothwell for inspiring me to do this thesis. I would also like to thank Brian Wright, Mark Perrin and Sumant Jayaraman for their observation and comments during the program development. Finally I would like to thank my wife Abhilasha for her infinite love and support.

TABLE OF CONTENTS

LIST OF FIGURES

CHAPTER 1

FIELD SOLUTIONS TO THE CAVITY PROBLEM

1.1 Introduction

The resonant fields inside microwave cavities have complex three dimensional patterns. It is sometimes quite difficult to mentally extrapolate these fields into three dimensions from two dimensional field plots illustrated in electromagnetic textbooks[2]. The following thesis develops a better way of visualizing and understanding these fields using a computer and its graphing capabilities.

Solving Maxwell's time harmonic equations inside a source free cylindrical cavity with perfectly conducting walls yields two sets of eigenmode solutions, namely the TE and TM modes [1]. The electric and magnetic field lines of these solutions have complex three dimensional field patterns. The field solutions can be solved on any two orthogonal planes cutting through the cavity. The three dimensional flow of these fields can then be interpreted by correlating the field pattern on the two planes [2]. This thesis attempts to make it even easier to visualize these fields by generating the field patterns in three dimensions in a computer and then projecting them onto the computer screen. The user is then given control to change his view point in real time to understand the complex flow of the field patterns. The program was written in Microsoft Visual C++™ and runs in the Microsoft Windows Operating System [3]. It also requires a math coprocessor and a display palette of at least 256 colors.

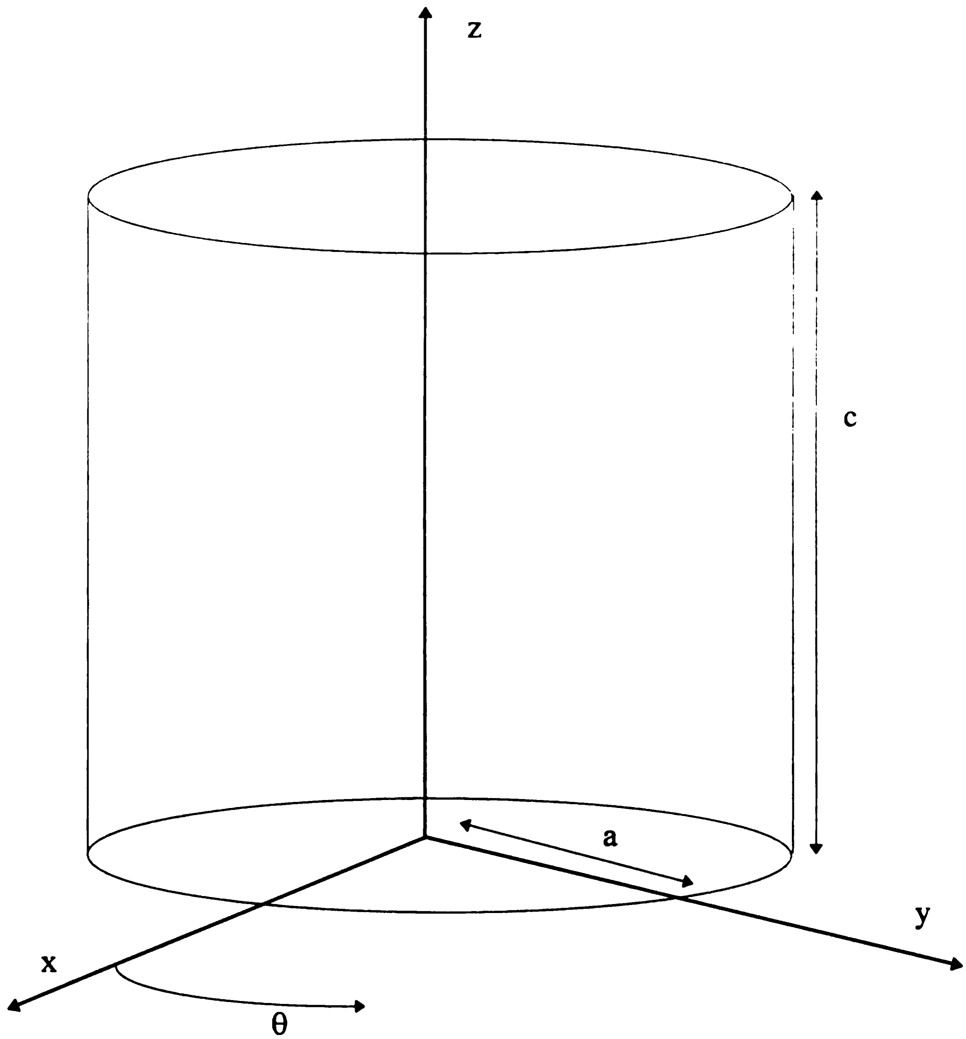

Figure 1. Cavity Model

1.2 TE or H modes

Consider the magnetic Hertz potential

$$\vec{\Pi}_h = \hat{z}\Pi_h \text{, where } \nabla^2\Pi_h + k^2\Pi_h = 0 \tag{1.1}$$

Solving the above partial differential equation by applying the following boundary conditions [1]

$\hat{n} \times \vec{E} = 0$ on $r = a$, $z = 0$ and $z = c$

gives,

$$\Pi_h(r,\theta,z) = AJ_n\left(\frac{p'_{nm}}{a}r\right)\begin{Bmatrix}\cos n\theta \\ \sin n\theta\end{Bmatrix}\sin\left(\frac{l\pi}{c}z\right) \tag{1.2}$$

The electric and magnetic fields can then be obtained using the following two relations

$$\vec{E} = j\omega\mu\left(-\hat{r}\frac{1}{r}\frac{\partial\Pi_h}{\partial\theta} + \hat{\theta}\frac{\partial\Pi_h}{\partial r}\right) \tag{1.3}$$

$$\vec{H} = \hat{z}\left(k^2\Pi_h + \frac{\partial^2\Pi_h}{\partial z^2}\right) + \hat{r}\frac{\partial^2\Pi_h}{\partial r\partial z} + \hat{\theta}\frac{1}{r}\frac{\partial^2\Pi_h}{\partial\theta\partial z} \tag{1.4}$$

Substituting (1.2) in (1.3) and (1.4) yields the following set of TE_{nml} modal fields

$$E_r = j\omega\mu An\frac{1}{r}J_n\left(\frac{p'_{nm}}{a}r\right)\begin{Bmatrix}\sin n\theta \\ -\cos n\theta\end{Bmatrix}\sin\left(\frac{l\pi}{c}z\right) \tag{1.5}$$

$$E_\theta = j\omega\mu A\left(\frac{p'_{nm}}{a}\right)J'_n\left(\frac{p'_{nm}}{a}r\right)\begin{Bmatrix}\cos n\theta \\ \sin n\theta\end{Bmatrix}\sin\left(\frac{l\pi}{c}z\right) \tag{1.6}$$

$$H_r = A\left(\frac{p'_{nm}}{a}\right)\left(\frac{l\pi}{c}\right)J'_n\left(\frac{p'_{nm}}{a}r\right)\begin{Bmatrix}\cos n\theta \\ \sin n\theta\end{Bmatrix}\cos\left(\frac{l\pi}{c}z\right) \tag{1.7}$$

$$H_\theta = -An\left(\frac{l\pi}{c}\right)\frac{1}{r}J_n\left(\frac{p'_{nm}}{a}r\right)\begin{Bmatrix}\sin n\theta \\ -\cos n\theta\end{Bmatrix}\cos\left(\frac{l\pi}{c}z\right) \tag{1.8}$$

$$H_z = A\left(k^2 - \left(\frac{l\pi}{c}\right)^2\right) J_n\left(\frac{p'_{nm}}{a} r\right)\begin{Bmatrix}\cos n\theta \\ \sin n\theta\end{Bmatrix}\sin\left(\frac{l\pi}{c} z\right) \tag{1.9}$$

The resonant frequency is given by

$$f_{nml} = \frac{\upsilon_c}{2\pi}\sqrt{\left(\frac{p'_{nm}}{a}\right)^2 + \left(\frac{l\pi}{c}\right)^2} \tag{1.10}$$

where n,m and l stand for the order of modes along θ, r, z coordinates and k, p'_{nm} and v_c stand for the wavenumber,zeros of bessel primes and velocity of light respectively.

1.3 TM or E modes

Consider the electric Hertz potential

$$\vec{\Pi}_e = \hat{z}\Pi_e \text{ , where } \nabla^2\Pi_e + k^2\Pi_e = 0 \tag{1.11}$$

Solving the above partial differential equation by applying the following boundary conditions [1]

$\hat{n} \times \vec{E} = 0$ on $r = a$, $z = 0$ and $z = c$

gives

$$\Pi_e(r,\theta,z) = BJ_n\left(\frac{p_{nm}}{a} r\right)\begin{Bmatrix}\cos n\theta \\ \sin n\theta\end{Bmatrix}\cos\left(\frac{l\pi}{c} z\right) \tag{1.12}$$

The magnetic and electric fields can then be obtained using the following two relations

$$\vec{H} = j\omega\varepsilon\left(\hat{r}\frac{1}{r}\frac{\partial\Pi_e}{\partial\theta} - \hat{\theta}\frac{\partial\Pi_e}{\partial r}\right) \tag{1.13}$$

$$\vec{E} = \hat{z}\left(k^2 + \frac{\partial^2\Pi_e}{\partial z^2}\right) + \hat{r}\frac{\partial^2\Pi_e}{\partial r\partial z} + \hat{\theta}\frac{1}{r}\frac{\partial^2\Pi_e}{\partial\theta\partial z} \tag{1.14}$$

Substituting (1.12) in (1.13) and (1.14) yields the following set of TM_{nml} modal fields

$$E_r = -B\left(\frac{p_{nm}}{a}\right)\left(\frac{l\pi}{c}\right)J_n'\left(\frac{p_{nm}}{a}r\right)\begin{Bmatrix}\cos n\theta\\ \sin n\theta\end{Bmatrix}\sin\left(\frac{l\pi}{c}z\right) \tag{1.15}$$

$$E_\theta = Bn\left(\frac{l\pi}{c}\right)\frac{1}{r}J_n\left(\frac{p_{nm}}{a}r\right)\begin{Bmatrix}\sin n\theta\\ -\cos n\theta\end{Bmatrix}\sin\left(\frac{l\pi}{c}z\right) \tag{1.16}$$

$$E_z = B\left(k^2 - \left(\frac{l\pi}{c}\right)^2\right)J_n\left(\frac{p_{nm}}{a}r\right)\begin{Bmatrix}\cos n\theta\\ \sin n\theta\end{Bmatrix}\cos\left(\frac{l\pi}{c}z\right) \tag{1.17}$$

$$H_r = -j\omega\varepsilon n\frac{1}{r}J_n\left(\frac{p_{nm}}{a}r\right)\begin{Bmatrix}\sin n\theta\\ -\cos n\theta\end{Bmatrix}\cos\left(\frac{l\pi}{c}z\right) \tag{1.18}$$

$$H_\theta = -j\omega\varepsilon\left(\frac{p_{nm}}{a}\right)J_n'\left(\frac{p_{nm}}{a}r\right)\begin{Bmatrix}\cos n\theta\\ \sin n\theta\end{Bmatrix}\cos\left(\frac{l\pi}{c}z\right) \tag{1.19}$$

The resonant frequency is given by

$$f_{nml} = \frac{\upsilon_c}{2\pi}\sqrt{\left(\frac{p_{nm}}{a}\right)^2 + \left(\frac{l\pi}{c}\right)^2} \tag{1.20}$$

where n,m and l stand for the order of modes along θ, r, z coordinates and k, p'_{nm} and v_c stand for the wavenumber,zeros of bessel function and velocity of light respectively.

The above set of equations completely describe the resonant electric and magnetic fields inside an ideal unloaded cylindrical cavity. The next chapter will deal with a little bit of background in three dimensional transformation and projection required by the program to compute these field patterns.

CHAPTER 2

THREE DIMENSIONAL TRANSFORMATION

2.1 Three Dimensional Transformational Matrices

Rotation of any point in three dimensions about the origin for an arbitrary angle can be accomplished by a sequence of rotations about the X,Y and Z axis. The following set of matrices describe the rotational transformation that can be applied to a point in three dimensions [4].

Rotational transform for any point in the X-Y plane is given by

$$R_{xy}(\theta) = \begin{bmatrix} \cos\theta & -\sin\theta & 0 & 0 \\ \sin\theta & \cos\theta & 0 & 0 \\ 0 & 0 & 1 & 0 \\ 0 & 0 & 0 & 1 \end{bmatrix}$$

Similarly, the rotational transform of Y-Z and X-Z planes are given by

$$R_{yz}(\theta) = \begin{bmatrix} 0 & 0 & 0 & 0 \\ 0 & \cos\theta & -\sin\theta & 0 \\ 0 & \sin\theta & \cos\theta & 0 \\ 0 & 0 & 0 & 1 \end{bmatrix} \qquad R_{xz}(\theta) = \begin{bmatrix} \cos\theta & 0 & -\sin\theta & 0 \\ 0 & 1 & 0 & 0 \\ \sin\theta & 0 & \cos\theta & 0 \\ 0 & 0 & 0 & 1 \end{bmatrix}$$

The following example gives us an idea on how these matrices could be used.

$$\begin{bmatrix} X' \\ Y' \\ Z' \\ 1 \end{bmatrix} = R_{xy}(45^\circ) \cdot R_{yz}(35^\circ) \cdot R_{xz}(25^\circ) \cdot \begin{bmatrix} X \\ Y \\ Z \\ 1 \end{bmatrix}$$

The above equation would rotate a point (X,Y,Z) on X-Z first, then followed by Y-Z and X-Y respectively to give (X', Y', Z')

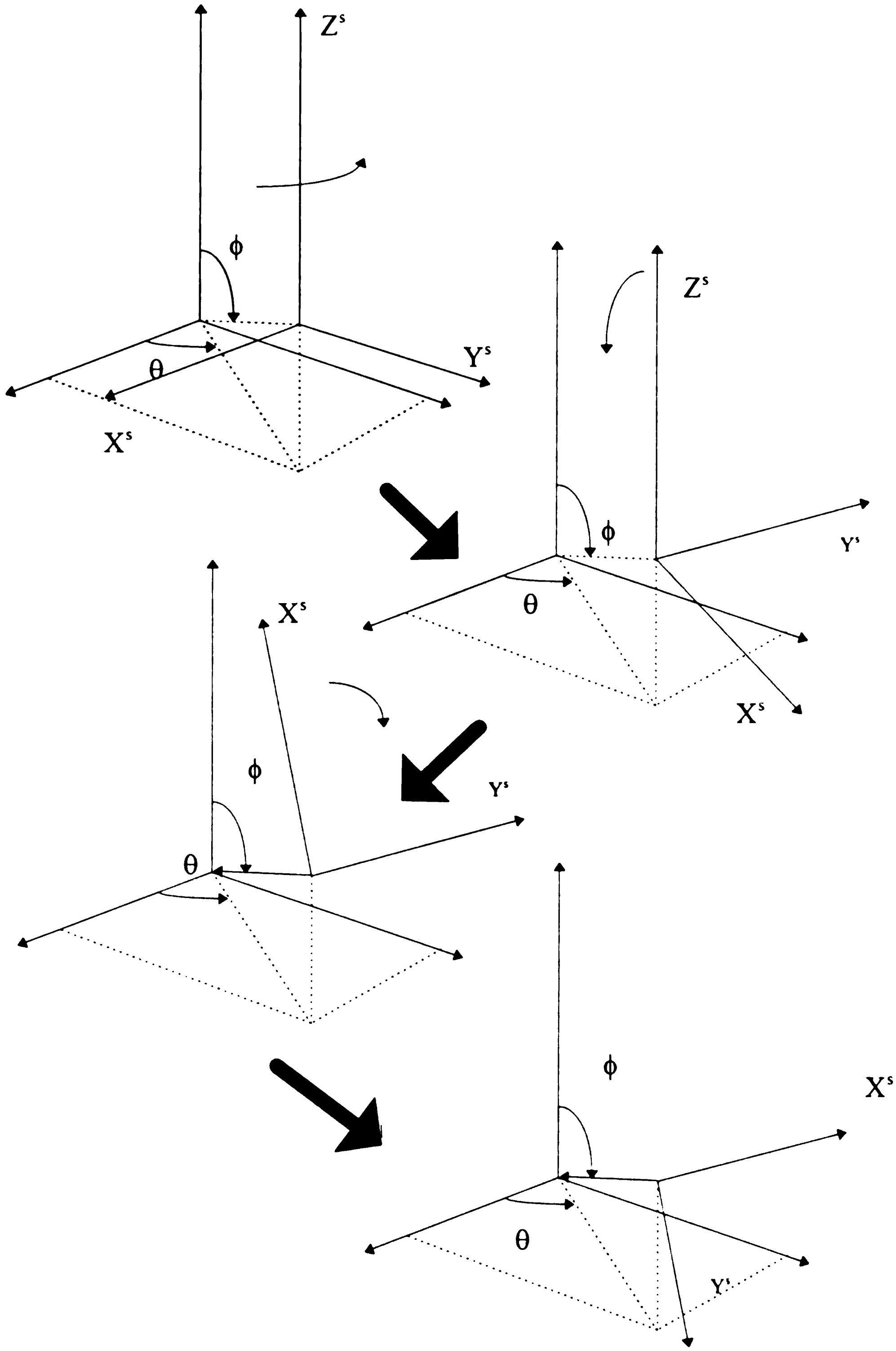

Figure 2.1 Rotation Sequence of the Reference Frame

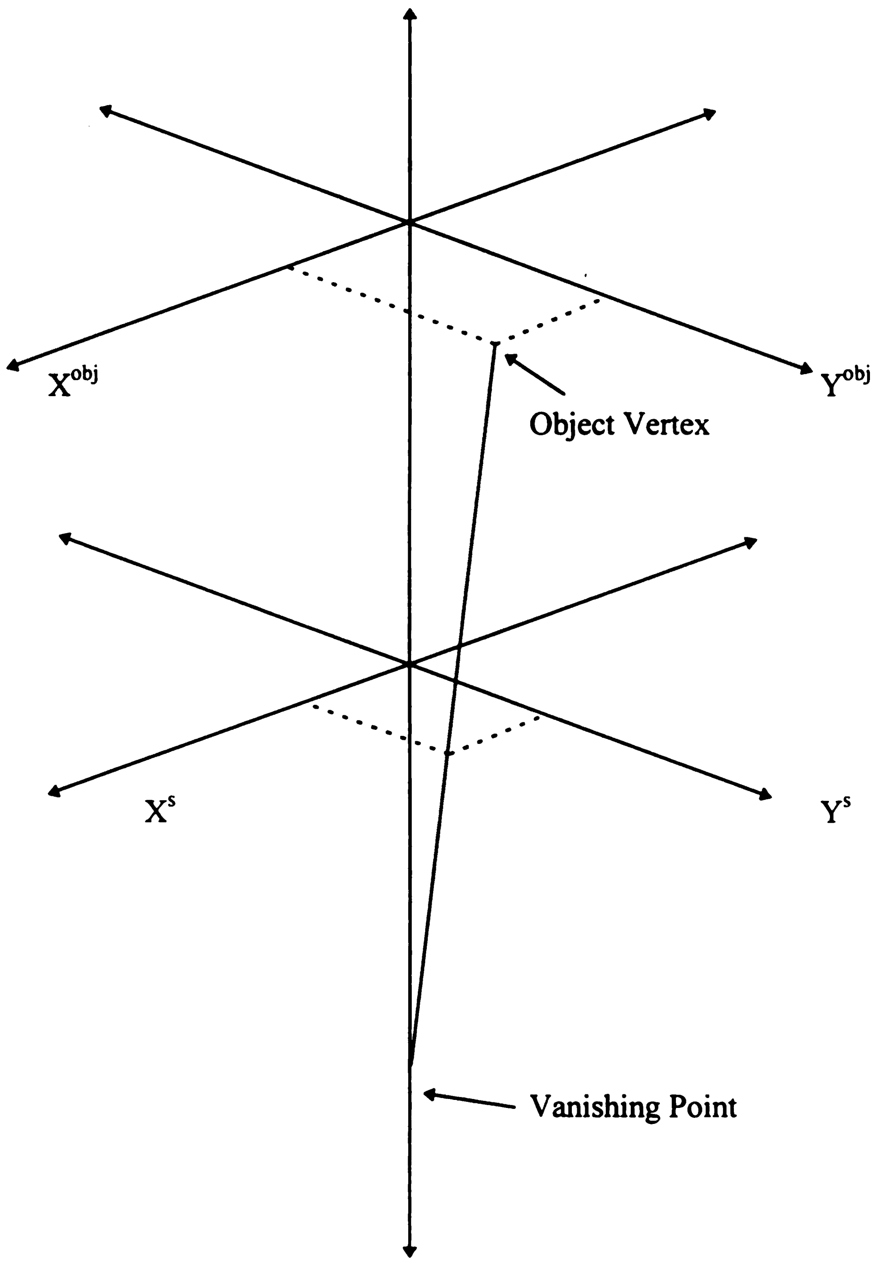

Figure 2.2 Two Dimensional Projection Scheme

2.2 Fundamentals of Two Dimensional Projection

The procedure used in finding the two dimensional projection of the vertices of an object centered at the origin requires a sequence of rotations followed by a translation operation be performed on each vertex of the object before projecting it onto a plane. Here the X-Y plane is used as the projection plane the orientation of which corresponds to the X and Y axis of the computer screen. In the sequence of rotations shown in Fig 2.1 the X^s-Y^s plane is rotated and translated to a view point specified in spherical coordinates. In the orientation shown in Figure 2.2 the object can then be projected onto the X^S-Y^S plane quite easily by employing a vanishing point located on the Z^S axis as follows

$$X^S = S \cdot \frac{(VNPT)}{(VNPT + Z^{obj})} \cdot X^{obj} + X_{Offset} \tag{2.1}$$

$$Y^S = S \cdot \frac{(VNPT)}{(VNPT + Z^{obj})} \cdot Y^{obj} + Y_{Offset} \tag{2.2}$$

S=Scale Factor	$X_{Offset}=Y_{Offset}$=Center Offset
VNPT=Vanishing Point	$(X^{obj}, Y^{obj}, Z^{obj})$=A Vertex on the Object

The purpose of the vanishing point is to add perspective to the projected image and the offset for centering the image on the computer screen. It is important to note that the view point angles entered by the user are the camera coordinates and hence the negative of the input angles should be used in all of the rotations shown in Fig 2.1. This results in the following equation

$$\begin{bmatrix} X' \\ Y' \\ Z' \\ 1 \end{bmatrix} = R_{xy}(-\theta) \cdot R_{xz}(-(180-\phi)) \cdot R_{xy}(-90^\circ) \cdot \begin{bmatrix} X \\ Y \\ Z \\ 1 \end{bmatrix}$$

$$\begin{bmatrix} X' \\ Y' \\ Z' \\ 1 \end{bmatrix} = \begin{bmatrix} -\sin\theta & \cos\theta & 0 & 0 \\ \cos\theta\cos\phi & \sin\theta\cos\phi & -\sin\phi & 0 \\ -\cos\theta\sin\phi & -\sin\theta\sin\phi & -\cos\phi & 0 \\ 0 & 0 & 0 & 1 \end{bmatrix} \cdot \begin{bmatrix} X \\ Y \\ Z \\ 1 \end{bmatrix} \qquad (2.3)$$

Equation (2.3) represents the transformation required to orient the computer screen or the camera toward the origin as shown in Fig 2.1. Applying equations (2.1) and (2.2) to (2.3) will yield the two dimensional projection of a three dimensional object centered around the origin.

CHAPTER 3

GENERATION OF FIELD AND INTENSITY

3.1 Cavity Geometry

The cavity model as shown in Figure 1 used by the program has the following geometry

a = 10cm, c = 20cm

Depending on the mode the user requests the field patterns are computed using either equations (1.5)-(1.9) or equations (1.15)-(1.19) using the resonant frequency computed by either equation (1.10) or equation (1.20) for the above cavity dimension.

3.2 Generation of Field Patterns

The volume shown in Figure 3 is inside the cavity and is bounded by the surfaces described by their normals. The electric and magnetic fields are then generated from points on these surfaces. The field direction is computed on a point on the surface and is used to compute the next point a finite distance in that direction. This procedure is repeated until the point reaches any one of the bounding surfaces. If the field happens to point away from the volume at any one of the starting surfaces the points are then back traced to fill the volume. The surfaces and the density of lines can be specified as inputs to the program. The program will then compute the field lines and display them on the computer screen. The user can then can move the view point in spherical coordinates around the cylinder to visualize the fields.

3.3 Generation of Field Intensities

The intensity of the fields can be generated along either the z = constant plane or the θ=constant plane. The intensity values are then scaled to an *hsv* color map that ranges

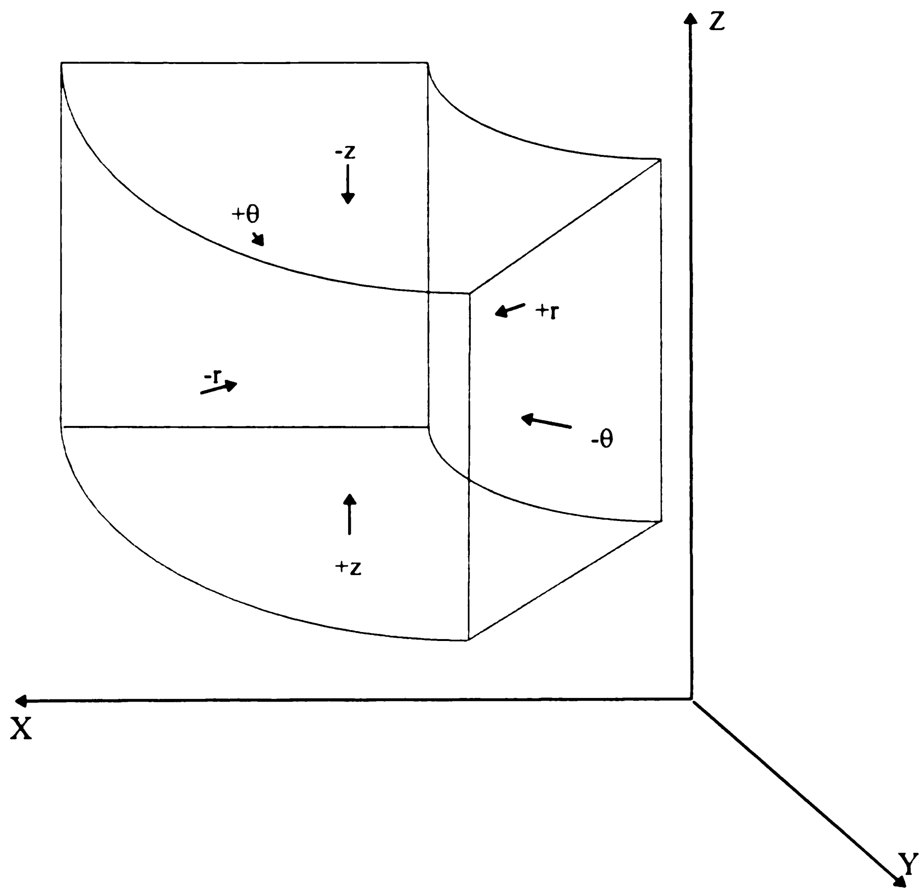

Figure 3 Input Volume Slice

from purple(highest) to green(medium) to red(lowest). The slice is then superimposed on the cylinder and displayed in three dimensions. As in the case of viewing field trajectories the view point of the user can then be moved around the cylinder to visualize the slices.

3.4 Limitations of the current version of the software

It is important to note that the scaled range of values for the intensity plot is relative to the intensities on the input plane. It does not take into account the maximum or the minimum field intensity in the entire cavity. An analytical solution to the maximum field intensity in the entire cavity could be derived to scale the intensity values. The next version of the software will address this problem. In the mean time inspection of both the z-slice and the theta-slice is enough give a good idea of the field intensity distribution in the entire cavity. There is also a limit set on the highest mode the program can handle in its current form. This was set because of the limitations in the computing speed and screen resolution available on a typical run-of-the-mill computer currently accessible to a student.

3.5 Future Modifications

The future version of this software will incorporate better shading algorithms to include translucent color surfaces and other surface rendering algorithms to enhance the quality of the display subroutines [5]. The use of three dimensional synchronized polarized glasses is also another possibility to give a virtual reality feel to the viewing environment [6].

LIST OF REFERENCES

LIST OF REFERENCES

[1] K. Chen, Electromagnetic Fields and Waves II, Class Notes, Department of Electrical Engineering, Michigan State University, p116-p124, (1993).

[2] S. Ramo, Fields and waves in communication electronics. New York: Wiley (1994).

[3] D. Kruglinski, Inside Visual C++™, Microsoft Press, Second Edition.

[4] R. Hill, Elementary linear algebra with applications. Fort Worth: Harcourt Brace Jovanovich, Second Edition, (1991).

[5] Foley, VanDam, Feiner & Hughes, Computer Graphics/Principles and Practice, Addison-Wesley, Second Edition.

[6] D. Stampe, B. Roehl & J. Eagan, Virtual Reality Creations. The Waite Group, (1993).

APPENDIX

SAMPLE MAGNITUDE OUTPUT FROM THE PROGRAM